Project Report (Group No 9)
Design of an NPC DAB for EV battery charging System (EE-665 Jan-May 2024)

submitted

by

Name: P.Mouni Rishitha Roll No 234102110

Name: P.Venkatadri Roll No 234102111

Under the instruction and guidance of

Dr Chandan Kumar

Department of Electronics and Electrical Engineering
Indian Institute of Technology Guwahati
May 7th 2024

Contents

1 Contribution

1.1 Name:P.Mouni Rishitha

- Visio(Fig-1, Fig-2,Fig-5)
- Literature Survey (ref-1,3)
- Operation of DAB and NPC DAB
- Power Flow analysis of NPC DAB
- Open Loop of NPC DAB
- Closed loop and Visio Diagrams and graphs
- Closed loop simulaiton of lithium ion Battery

1.2 Name:P.Venkatadri

- Control Techniques, Introduction
- working states of npc
- Visio (Fig-4, Fig-3)
- Literature Survey (ref-2,4,5)
- Calculations of NPC DAB
- Closed Loop of NPC DAB
- Open Loop and Visio Diagrams and graphs
- Open loop simulaiton of lithium ion Battery

2 Origin of the Dual Active Bridge (DAB) converter :

The Dual Active Bridge (DAB)converter is a widely used electronic power converter in the field of electricity and high voltage. Its primary function is to convert energy between two phases of electricity, making it highly suitable for applications such as electric vehicle charging, renewable energy, and high voltage operations. [1]
The typical design of a dual active bridge converter consists of two sets of power electronic switches, usually MOSFETs or IGBTs, arranged in a bridge configuration along with a separate transformer. This unique arrangement enables the converter to facilitate bi-directional power flow while ensuring safety and reliability through galvanic isolation between the input and output. One of the standout features of DAB converters is their ability to deliver exceptional performance and efficiency, thanks to advanced control mechanisms. By precisely controlling the duration and amplitude of the conversion signal, these converters can minimize losses and maximize power conversion in various functions. Furthermore, DAB converters offer great flexibility in terms of voltageand power conversion, allowing them to cater to diverse requirements. This adaptability makes them highly suitable for a wide range of applications, including grid-connected renewable energy systems, electric power applications, and multi-electric vehicle operations. [2]
Conversion applications that offer a two-way power supply, electrical insulation, excellent efficiency, and user-friendly interface, among other benefits.

2.1 Advantages over traditional buck-boost converters:

- **Bidirectional Power Flow**:
  - Can transfer power efficiently in both directions.
  - Useful for applications requiring energy transfer between different voltage sources or storage systems.
- **High Efficiency**:
  - Achieves high efficiency over a wide range of operating conditions.
  - Minimizes switching losses through synchronous rectification and advanced control techniques.
- **Reduced Stress on Components**:
  - Distributes voltage and current stresses across multiple switches and transformer windings.
  - Enhances reliability and extends component lifespan, particularly in high-power applications.

- **Flexible Voltage Conversion Ratio**:
  - Offers flexibility in voltage conversion ratio by adjusting phase-shift angle.
  - Eliminates the need for multiple converter stages.
- **Improved Power Quality**:
  - Reduces harmonic distortion and ripple in output voltage and current.
  - Mitigates power quality issues like voltage ripple, harmonics, and EMI.
- **Scalability**:
  - Easily paralleled or configured in multi-phase arrangements.
  - Suitable for a wide range of power levels and applications, allowing for modular design and easy expansion.

3 Control Techniques

In controlling techniques, the primary focus is on managing the phase shift between the output voltages of the two bridge converters. This adjustment facilitates power flow through the leakage inductance of the transformer. Regulating the phase shift enables effective control over power transfer, ensuring optimal system operation and performance.

3.1 Pulse Width Modulation (PWM)

- PWM is a widely used technique in DAB converters to control the average voltage or current delivered to the load. [3]
- It involves varying the width of the switching pulses applied to the converter's switches while maintaining a constant switching frequency.
- By adjusting the duty cycle of the PWM signals, precise regulation of output parameters such as voltage or current is achieved, making it suitable for high accuracy and efficiency applications.

3.2 Phase-Shift Control

- Phase-shift control involves adjusting the phase angle between the switching signals of the primary and secondary bridges in the DAB converter. [4]

- By controlling the phase shift, the converter can regulate the timing of power transfer between the input and output sides.
- This control technique is particularly useful for bidirectional power flow applications, allowing for smooth and precise regulation of power flow through the leakage inductance of the transformer.

In summary, PWM and phase-shift control are essential techniques employed in DAB converters to regulate power flow, voltage, and current. While PWM provides fine-grained control over output parameters, phase-shift control enables efficient bidirectional power flow and precise timing control. Combining these techniques allows for versatile and efficient operation of DAB converters in various applications. Advanced algorithms and control strategies are continuously being developed to further improve the performance and efficiency of dual active bridge converters.

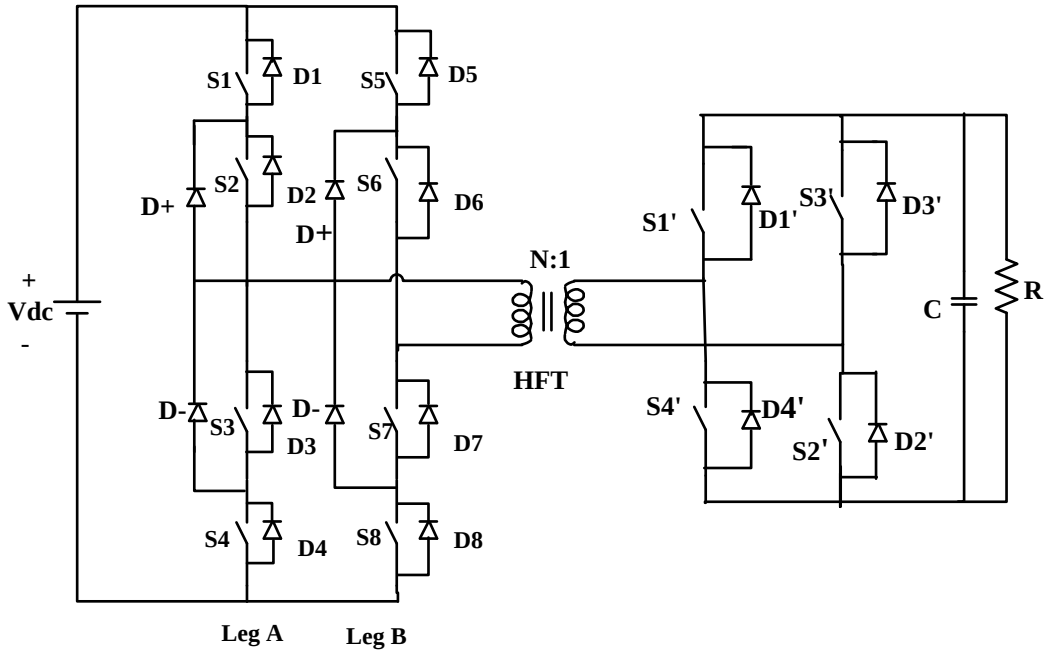

Figure 1: NPC DAB

4 Limitations of DAB Converter:

- Complex Control and Modeling.
- High Component Count and Cost.
- Efficiency at Light Loads.

- Voltage and Current Stress.
- Size and Weight.
- Limited Voltage and Power Range.
- EMI and Noise.

5 Neutral Point Clamp (NPC) Topology

The Neutral Point Clamp (NPC)topology is a cornerstone of modern power electronics, offering numerous benefits across various applications. One of its key advantages lies in its ability to mitigate voltage stress on switches. By providing multiple clamping points, NPC converters effectively limit voltage spikes, enhancing system reliability. [5]

Moreover, NPC topology plays a crucial role in minimizing switching losses. Through the distribution of voltage across multiple switches, it ensures that no individual switch experiences excessive stress during operation. This results in reduced power losses during switching transitions, leading to improved efficiency and energy conservation.

Additionally, NPC converters contribute significantly to better power quality. They are adept at reducing harmonic distortion in the output voltage waveform, which is essential for applications requiring clean and stable power supply, such as grid-connected renewable energy systems and industrial motor drives.

Furthermore, NPC topologies enhance the overall reliability of power conversion systems. The reduced stress on individual switches and improved voltage clamping mechanisms contribute to increased system robustness and reduced downtime, ultimately leading to cost savings for businesses. [5]

5.1 Objectives:

- **Improved Efficiency:** The NPC DAB converter is designed to achieve higher efficiency in power conversion. It minimizes power losses and enhances the overall efficiency of the system, making it suitable for applications where energy efficiency is crucial.
- **Improved Reliability:** The converter is designed for high reliability by minimizing stress on the power electronic components. The NPC configuration provides a balanced voltage across the clamping capacitors, reducing stress on the semiconductor devices and improving the overall reliability of the converter.
- **Grid Compatibility:** The NPC DAB converter aims to achieve compatibility with the grid requirements. It includes features to synchronize with the grid, maintain power factor correction, and adhere to grid codes and regulations.

5.2 Switching States of the 3L-NPC Bridge

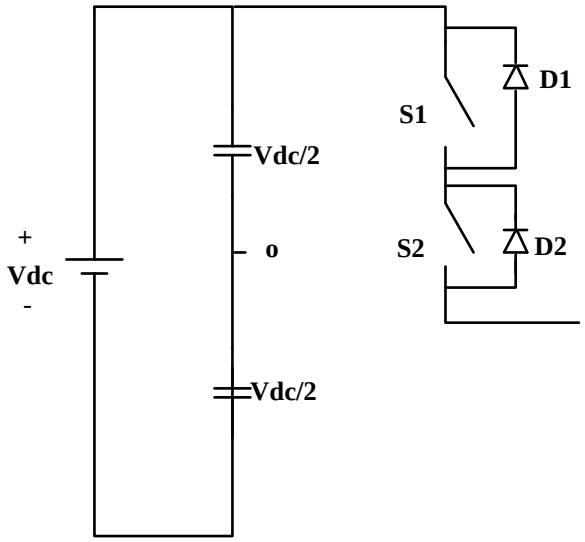

Figure 2: State 'P'

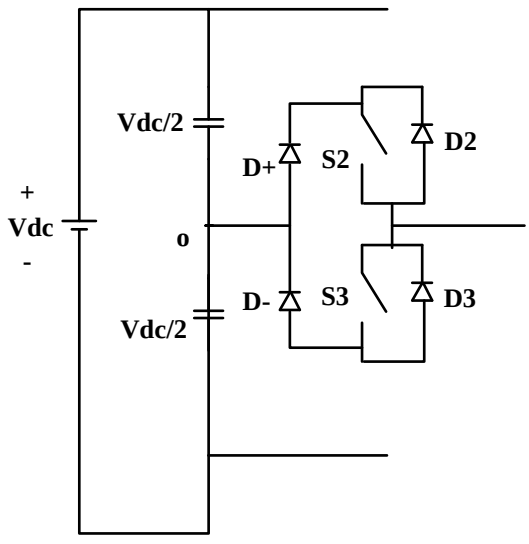

Figure 3: State 'O'

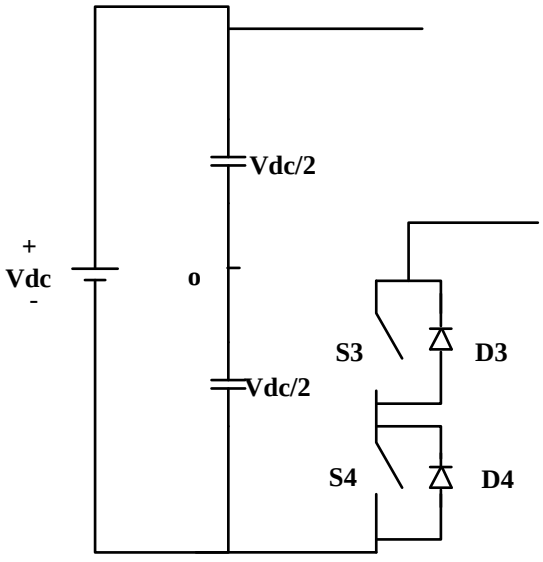

Figure 4: State 'N'

The Neutral Point Clamped (NPC) inverter was first introduced in 1980, leading to subsequent research into various aspects of the converter. These investigations have explored different

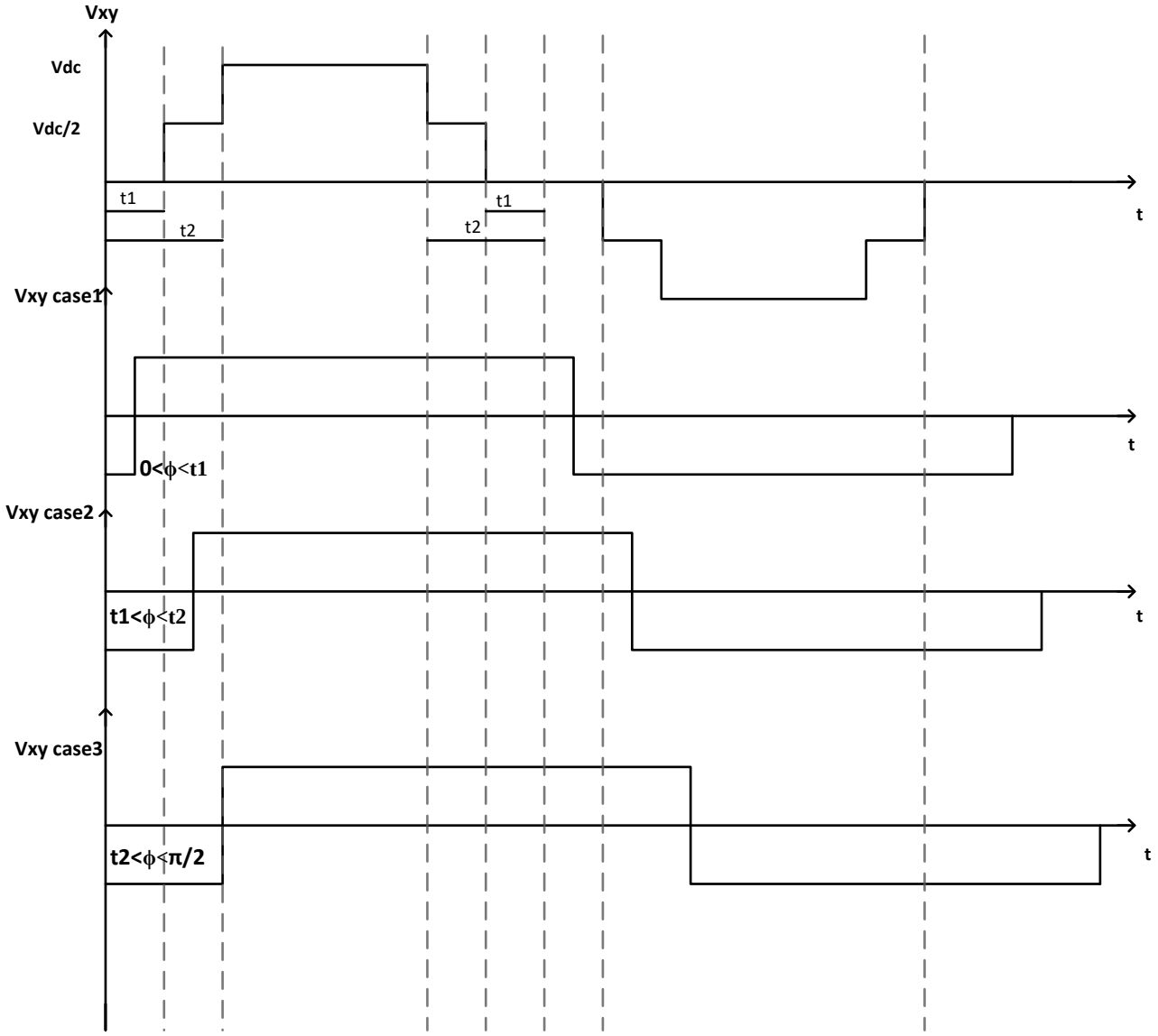

Figure 5: Waveforms of NPC DAB

modulation strategies, voltage level variations, capacitor voltage balancing techniques, harmonic reduction methods, and the utilization of active clamping instead of diodes. In the operational context of the NPC-DAB (Dual Active Bridge), the switching pattern of the NPC differs slightly from conventional inverters. Unlike 3L-NPC line frequency inverters, where the switching fre-

quency matches the line frequency, in NPC-DAB, the switching frequency corresponds to the fundamental frequency. The primary benefit of the 3L-NPC lies in the fact that, during state commutation, all switching devices in a leg experience only half of the DC bus voltage, resulting in reduced $\frac{dv}{dt}$ compared to a two-level inverter.However, the transition between "P" and "N" states involves all four switches in a leg during this scheme, with two switches being turned on and the other two being turned off. This process can result in varying dynamic voltages on each switch, potentially leading to double the switching losses. To address this issue, a small dead time is introduced between different states. The modulation strategy also extends to leg-Y, where a similar switching pattern is applied to generate a 3L voltage waveform. In this proposed modulation technique, the voltage V_{XO} is phase-shifted from $-V_{YO}$ by an amount (t1+t2) to create a voltage waveform (V_{XY}) across the transformer.

Table I: Switching States of Each NPC Leg

State	S1	S2	S3	S4	v_{XO}
P	On	On	Off	Off	$0.5V_{DC}$
O	Off	On	On	Off	0
N	Off	Off	On	On	$-0.5V_{DC}$

5.3 Mathematical Analysis of NPCDAB converter

Power Flow analysis of NPCDAB:

From the basic inductor current

$$v_L = L\frac{di_L}{d\theta}$$
$$\text{Or, } I_L = \frac{1}{\omega L}\int_{\theta_1}^{\theta_2} v_L\, d\theta \tag{1}$$

where $(\theta) = (\omega)t$.
For $0 < (\theta) < (\phi)$

$$i_L(\theta) = \frac{V_s}{\omega L}\theta + i_L(0)$$
$$i_L(\phi) = \frac{V_s}{\omega L}\phi + i_L(0) \tag{2}$$

For $(\phi) < (\theta) < t_1$

$$\begin{aligned} i_L(\theta) &= -\frac{V_s}{\omega L}(\theta) + i_L(\phi) \\ i_L(t_1) &= -\frac{V_s}{\omega L}(t_1 - \phi) + i_L(\phi) \end{aligned} \tag{3}$$

For $t_1 < (\theta) < t_2$

$$\begin{aligned} i_L(\theta) &= -\left(\frac{V_s - \frac{V_p}{2n}}{\omega L}\right)\theta + i_L(t_1) \\ i_L(t_2) &= -\left(\frac{V_s - \frac{V_p}{2n}}{\omega L}\right)(t_2 - t_1) + i_L(t_1) \end{aligned} \tag{4}$$

For $t_2 < \theta < (\pi - t_2)$

$$\begin{aligned} i_L(\theta) &= -\left(\frac{V_p - V_s}{\omega L}\right)\theta + i_L(t_2) \\ i_L(\pi - t_2) &= -\left(\frac{V_p - V_s}{\omega L}\right)(\pi - 2t_2) + i_L(t_2) \end{aligned} \tag{5}$$

For $(\pi - t_2) < \theta < (\pi - t_1)$

$$\begin{aligned} i_L(\theta) &= -\left(\frac{V_s - \frac{V_p}{2n}}{\omega L}\right)\theta + i_L(\pi - t_2) \\ i_L(\pi - t_1) &= -\left(\frac{V_s - \frac{V_p}{2n}}{\omega L}\right)(t_2 - t_1) + i_L(\pi - t_2) \end{aligned} \tag{6}$$

For $(\pi - t_1) < \theta < \pi$

$$\begin{aligned} i_L(\theta) &= -\left(\frac{V_s}{\omega L}\right)\theta + i_L(\pi - t_1) \\ i_L(\pi) &= -\left(\frac{V_s}{\omega L}\right)(t_1) + i_L(\pi - t_1) \end{aligned} \tag{7}$$

Assuming zero average current through the transformer

$$i_L(0) = -i_L(\pi) \tag{8}$$

After solving,

$$i_L(0) = \frac{V_p}{\omega L}\left(\frac{\pi}{2} - \alpha\right) - \frac{V_s}{\omega L}\left(\frac{\pi}{2} - \phi\right) \tag{9}$$

Putting this expression of $i_L(0)$ in the above equations, we can get the $i_L(\theta)$ at any point.The average power flow equations from the primary to secondary bridge through the leakage inductance

$$P_O = \frac{1}{\pi}\int_0^{\pi} V_{AB}(\theta) \cdot i_L(\theta)\, d\theta \tag{10}$$

Case 1:

$$P_O = \frac{V_p \cdot V_s}{n\omega L} \cdot \phi\left(1 - \frac{t_1}{\pi} - \frac{t_2}{\pi}\right); \quad 0 < \theta \leq t_1 \tag{11}$$

Case 2:

$$P_O = \frac{V_p \cdot V_s}{n\omega L}\left(\phi - \frac{\phi^2}{\pi} - \frac{t_1^2}{2\pi} - \frac{t_1 t_2}{\pi}\right); \quad t_1 < \theta \leq t_2 \tag{12}$$

Case 3:

$$P_O = \frac{V_p \cdot V_s}{n\omega L}\left(\phi - \frac{\phi^2}{\pi} - \frac{t_1^2}{2\pi} - \frac{t_2^2}{2\pi}\right); \quad t_2 < \theta \leq \frac{\pi}{2} \tag{13}$$

6 Calculations of NPC DAB Parameters

Given parameters:

- Supply voltage (V_{dc}): 5 kV
- Battery voltage (V_{bat}): 96 V
- Battery capacity: 20 kWh
- Charging current (I_{ch}): 2 C

calculation of Power:

$$P_o = E \times I_o$$

$$P_o = 20,000 \times 2C$$

$$P_o = 40,000\,\mathrm{W}$$

6.1 Capacitor Current

The capacitor current (I_{cap}) is equal to the charging current:

$$I_{\text{cap}} = 2\,\mathrm{C}$$

6.2 Inductance (L):

$$P_O = \frac{V_p \cdot V_s}{n\omega L} \cdot \phi \left(1 - \frac{t_1}{\pi} - \frac{t_2}{\pi}\right)$$

In this equation: - P_O represents the output power. - V_p represents the primary voltage. - V_s represents the secondary voltage. - n represents the number of turns. - ω represents the angular frequency. - L represents the inductance. - ϕ represents the flux. - t_1 and t_2 are time variables.

$$P_O = 40KW\,\mathrm{W}$$

$$V_p = 5000\,\mathrm{V}$$

$$V_s = 96\,\mathrm{V}$$

$$n = \frac{5000}{96}$$

$$f = 20 \times 10^3\,\mathrm{Hz}$$

$$\phi = 18^\circ = 0.314\,\mathrm{rad}$$

$$t_1 = 30^\circ = \frac{\pi}{6}\,\mathrm{rad}$$

$$t_2 = 45^\circ = \frac{\pi}{4}\,\mathrm{rad}$$

First, let's calculate ω:

$$\omega = 2\pi f = 2\pi \times 20 \times 10^3\,\mathrm{rad/s}$$

$$\omega = 40\pi \times 10^3\,\mathrm{rad/s}$$

Given: $V_p = 5000$ V , $V_s = 96$ V ,$n = 52.08$,$\omega = 2\pi \times 20 \times 1000$ rad/s ,$P_O = 40000$ W , $\phi = 0.785$,$t_1 = 0.314$,$t_2 = 0.523$.

We use the formula:

$$L = \frac{V_p \cdot V_s}{n\omega P_O} \cdot \phi \left(1 - \frac{t_1}{\pi} - \frac{t_2}{\pi}\right)$$

Substituting the given values:

$$L = \frac{5000 \cdot 96}{52.08 \times 125663.706 \times 40000} \cdot 0.785 \left(1 - \frac{0.314}{\pi} - \frac{0.523}{\pi}\right)$$

So, the inductance L is approximately $0.336\,\mu$H.

Output Current and Charging Capacitor Current(I_{out}): Consider the ripple as 3%. Let's calculate the current (I_o) using the provided values:

- $P = 40$ kW (kilowatts)
- $V = 96$ V (volts)

Using the formula $I_o = \frac{P}{V}$:

$$I_o = \frac{40\,\text{kW}}{96\,\text{V}}$$

$$I_o = \frac{40000\,\text{W}}{96\,\text{V}}$$

$$I_o \approx 416.67\,\text{A}$$

So, the current (I_o) is approximately 416.67 amperes.

6.3 Charging Capacitor Value(C_{ch}):

To calculate the capacitance , we typically use the following equation:

$$C = \frac{I_{ch} \cdot D * T_{sw}}{\Delta V_{cap}}$$

Where: C is the capacitance. , I_o is the charging current. , T_{sw} is the switching period. , ΔV_{cap} is the voltage ripple across the capacitor.

First, let's calculate the switching period:

$$T_{sw} = \frac{1}{f} = \frac{1}{20 \times 10^3}\,\text{s}$$

Then, we can find the voltage ripple (for 3 percent)across the capacitor (ΔV_{cap}):

$$\Delta V_{cap} = 0.03 * V_{bat} = 2.88\,\text{V}$$

$$C = \frac{I_o \cdot D \cdot T_{sw}}{\Delta V_{cap}}$$

Given: $I_o = 416.67$ A (charging current) , $D = 0.1$ (duty cycle) ,$T_{sw} = \frac{1}{20000}$ s (switching period) , $\Delta V_{cap} = 2.88$ V (change in voltage across the capacitor during the charging period)

Substituting the given values:

$$C = \frac{416.67 \times 0.1 \times \frac{1}{20000}}{2.88}$$

$$C = \frac{416.67 \times 0.1 \times \frac{1}{20000}}{2.88}$$

$$C = \frac{416.67 \times 0.1 \times 5 \times 10^{-5}}{2.88}$$

$$C = \frac{2083.35 \times 5 \times 10^{-5}}{2.88}$$

$$C = \frac{104.1675 \times 10^{-5}}{2.88}$$

$$C = \frac{0.001041675}{2.88}$$

$$C \approx 0.723 \text{ mF}$$

6.4 Calculation of Resistance

To calculate resistance (R) using V_s^2/P_O, where V_s is the output voltage and P_O is the output power, we have:

$$R = \frac{V_s^2}{P_O}$$

Given:

- $V_s = 96$ V (output voltage)
- $P_O = 40000$ W (output power)

Using the formula $R = \frac{V_s^2}{P_O}$:

$$R = 0.2304$$

Table II: Parameters and Values

Parameter	Value
Primary Voltage	5000 V
Battery Voltage	96 V
Leakage Inductance	0.3367 μH
Capacitance (Load Side)	0.723 mF
Resistance	0.2304 Ω
Switching Frequency	20 kHz
Battery Capacity	20 kWh
Turns ratio (n)	52.08
Leakage Inductance for NPC-DAB transformer	0.5 mH
3-level NPC bridge IGBT's V_{CE}	$V_{CE} = 1750V(70\% \times \frac{V_p}{2})$
2-level PV side bridge IGBT's V_{CE}	$V_{CE} = 48V(49\% \times V_s)$
Charging Current	2 C-rated
Phase Shift (ϕ)	18 degrees
Switching States of Each NPC Leg	As provided in Table I

7 Simulation Diagram of Open Loop NPC-DAB

7.1 Open Loop Mode:

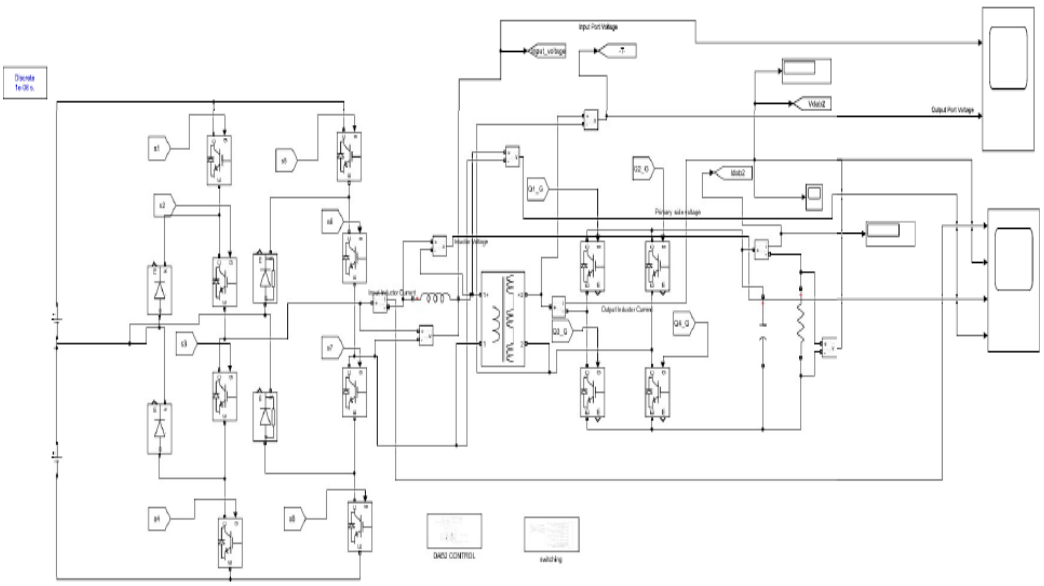

Figure 6: Simulation Diagram of Open Loop NPC-DAB

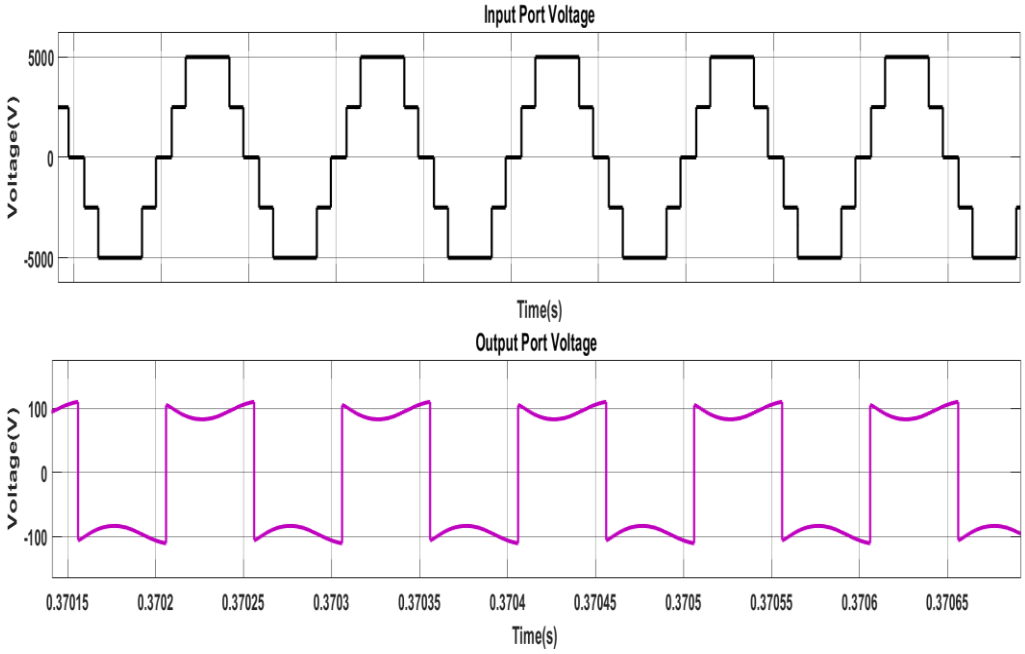

Figure 7: input output port Voltage graphs

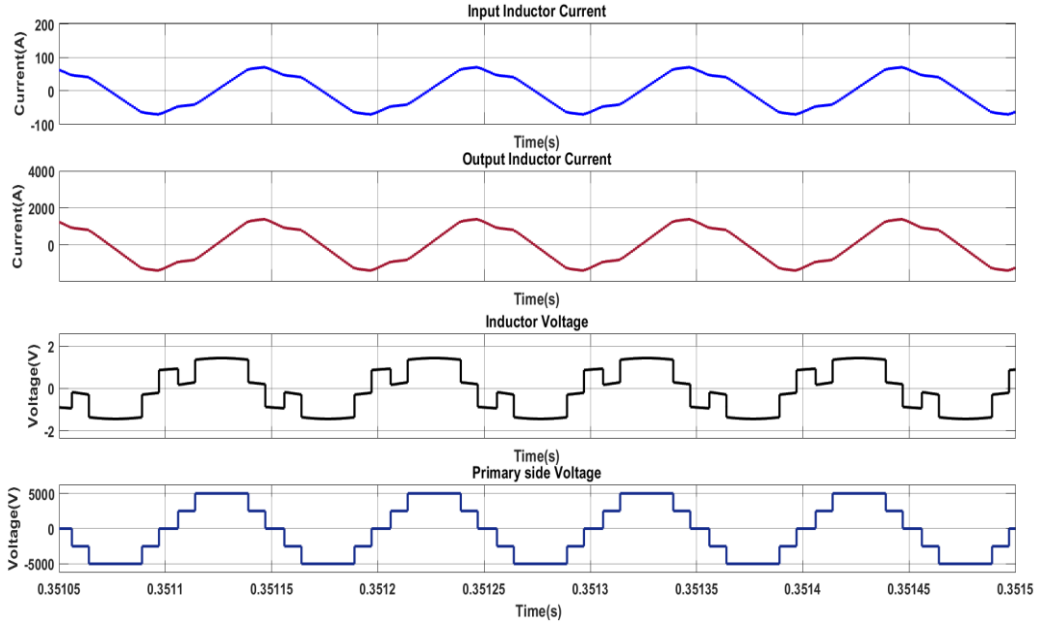

Figure 8: Inductor Current and Voltages

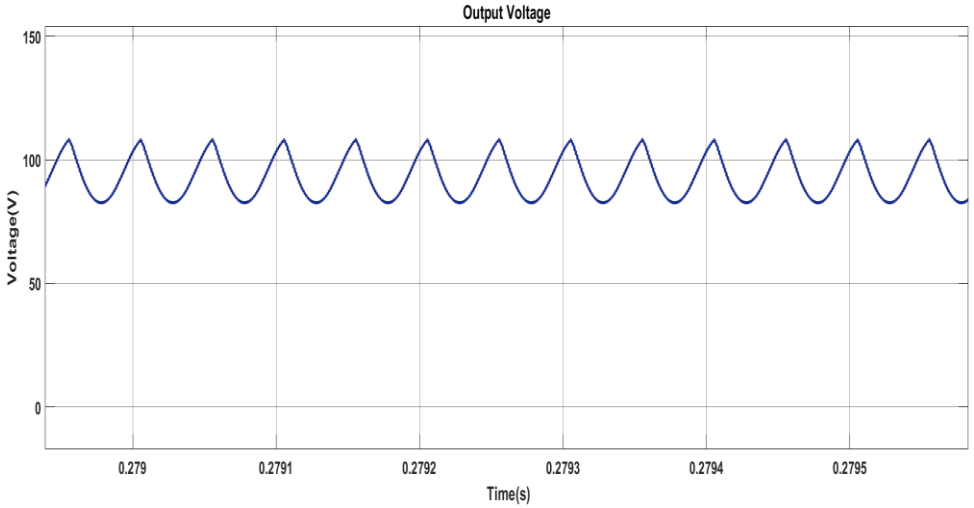

Figure 9: Output voltage

7.2 Closed Loop Control :

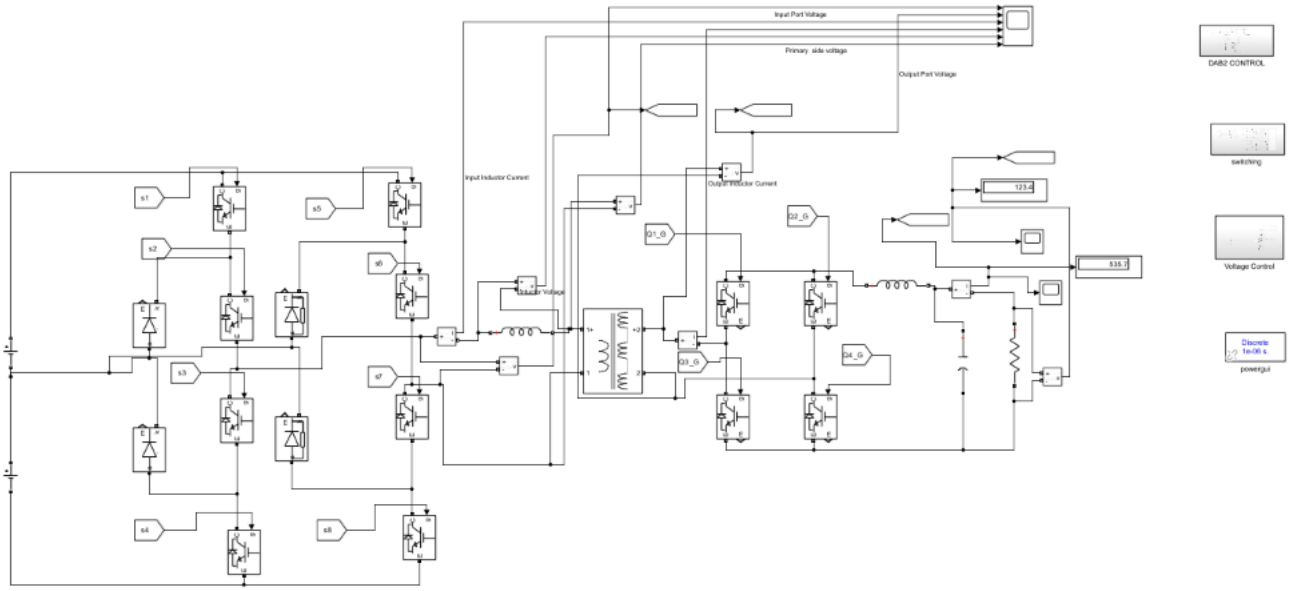

Figure 10: NPC-DAB Closed control Mode

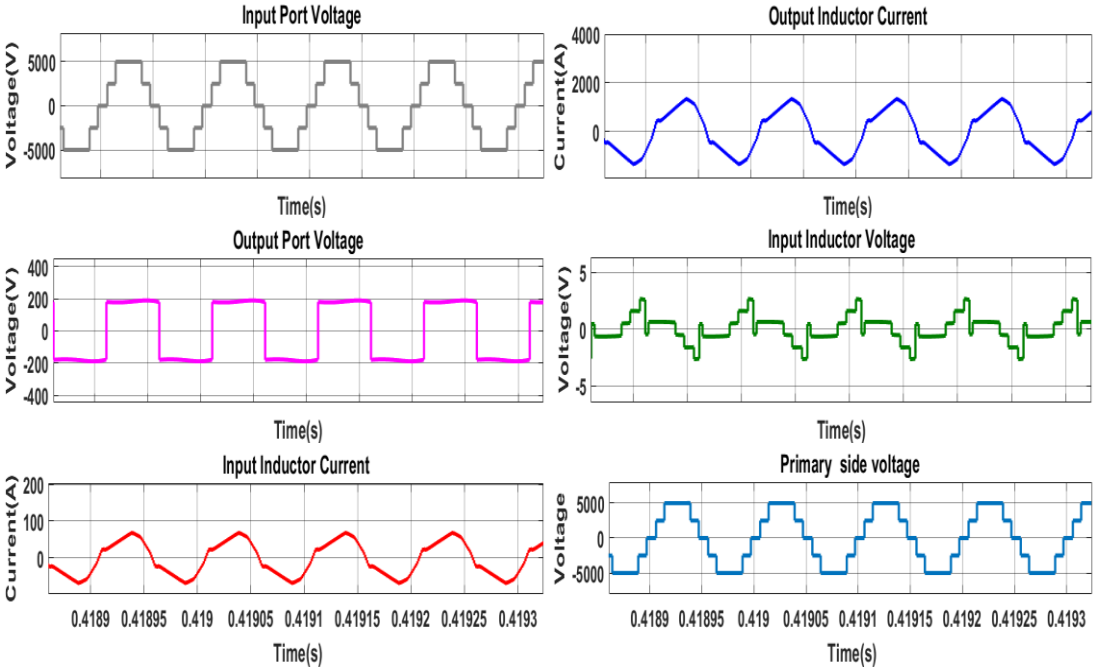

Figure 11: Input-output port Voltages and Currents

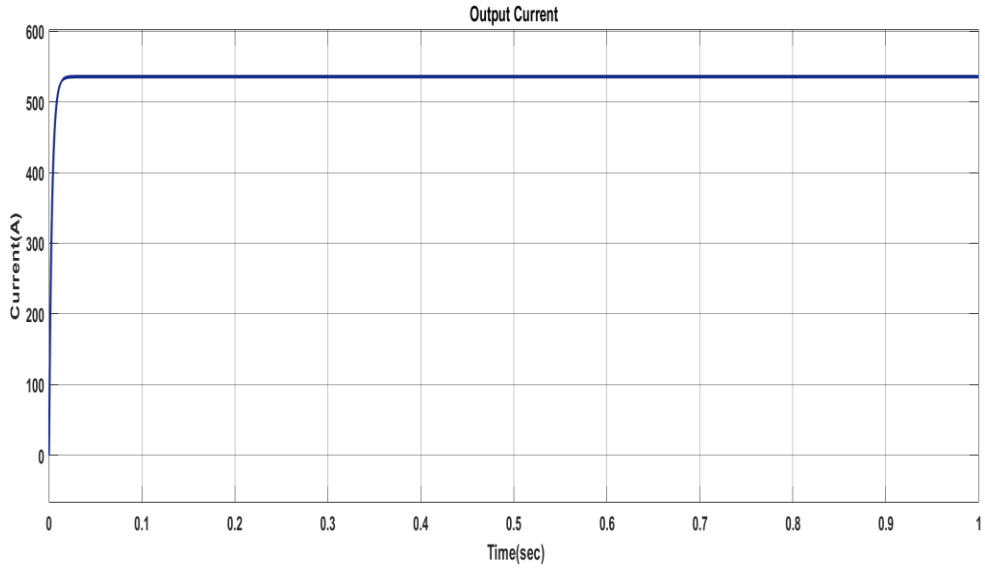

Figure 12: Output current

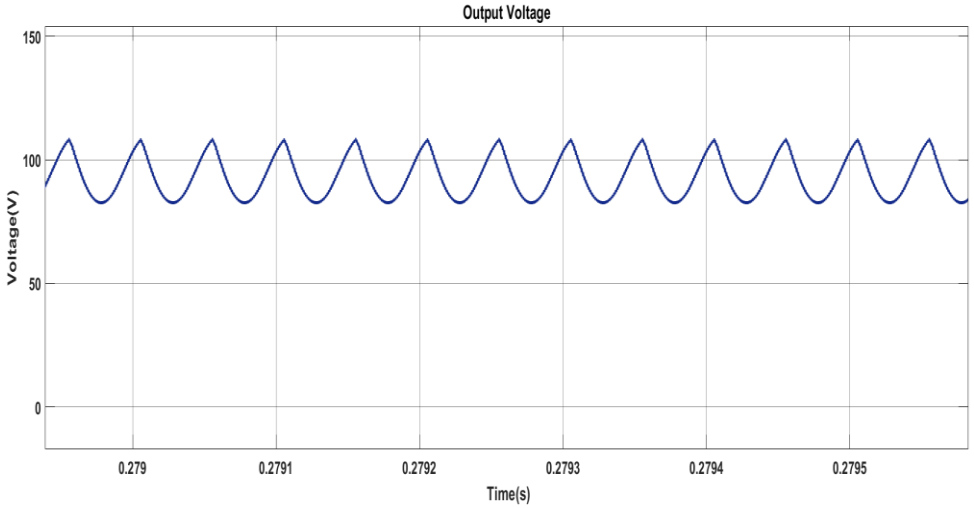

Figure 13: Output Voltage

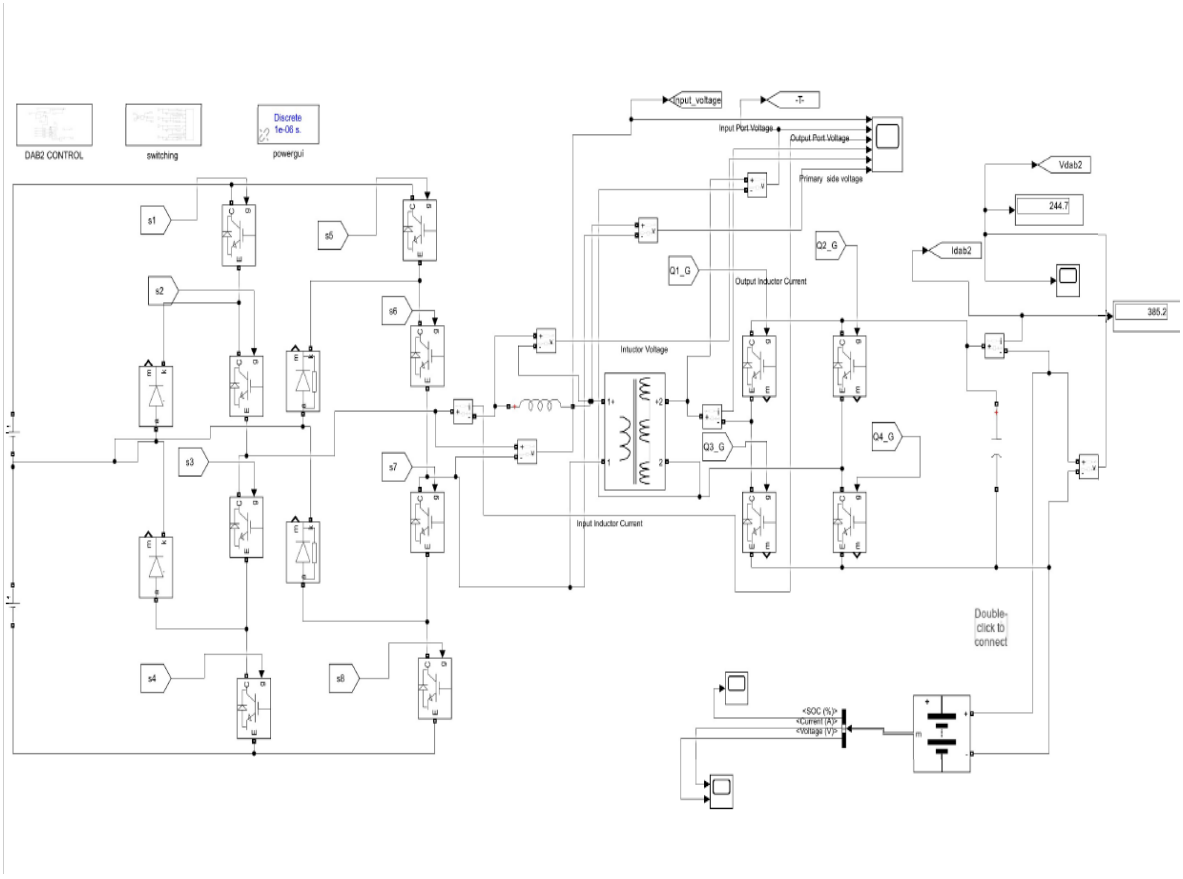

Figure 14: Simulation of Open loop charging of Lithium ion Battery

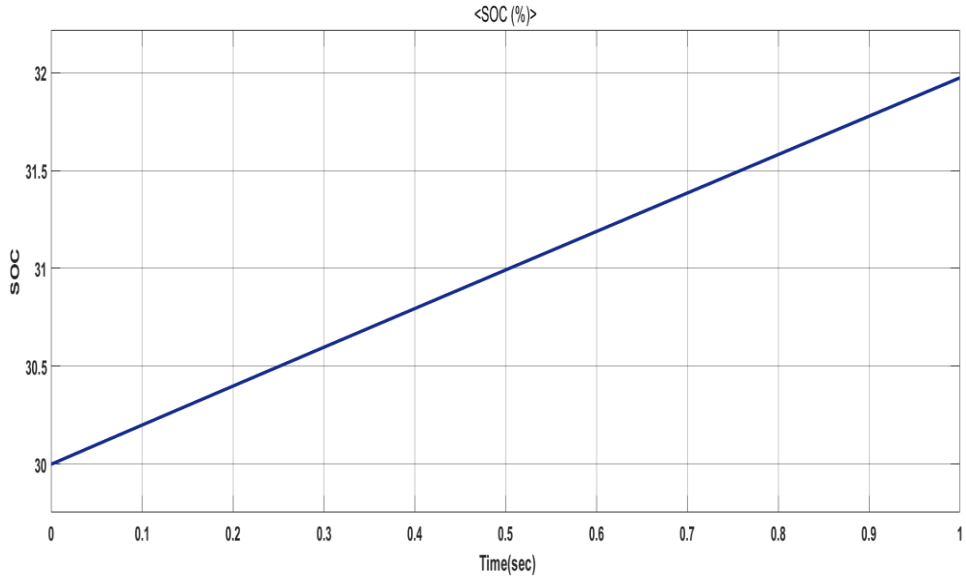

Figure 15: Percentage of SOC

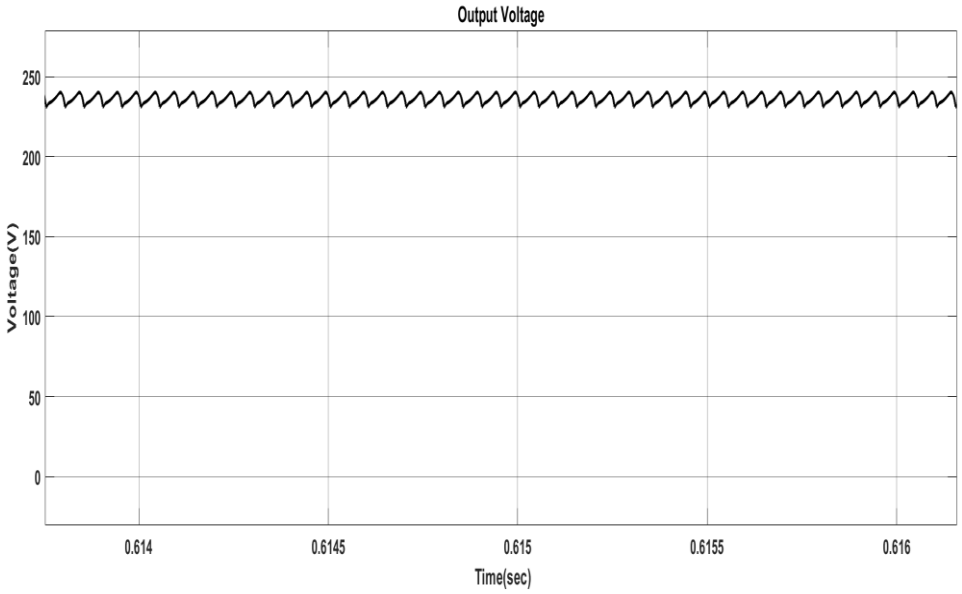

Figure 16: Output Voltage

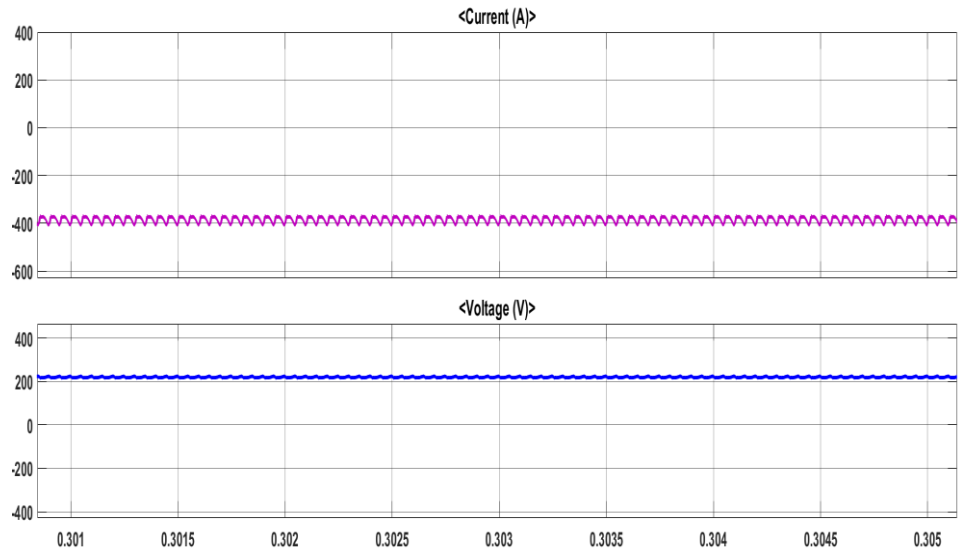

Figure 17: Voltage and Current of lithium ion Battery

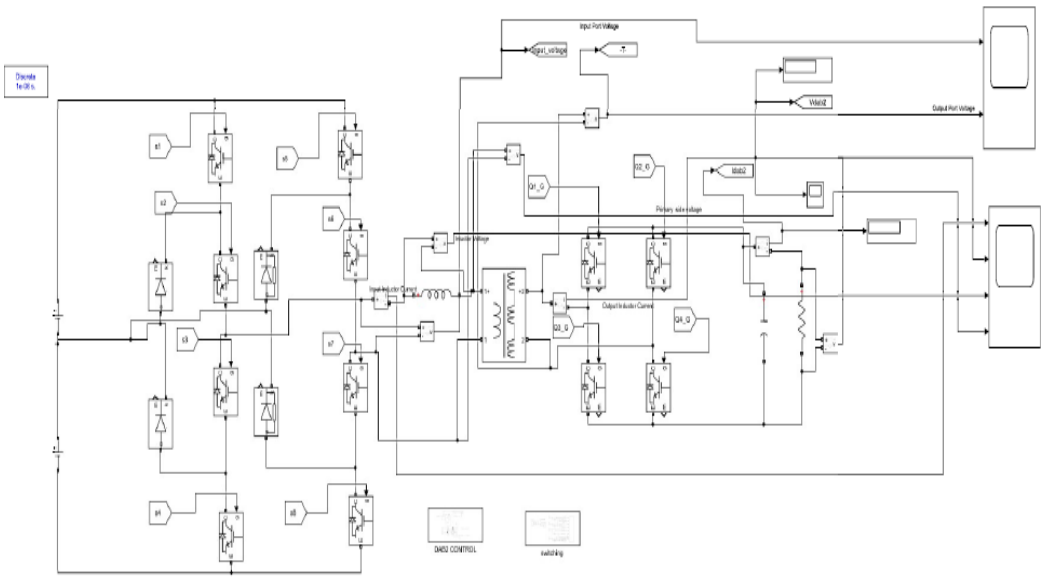

Figure 18: Simulation of charging of lithium ion battery closed loop

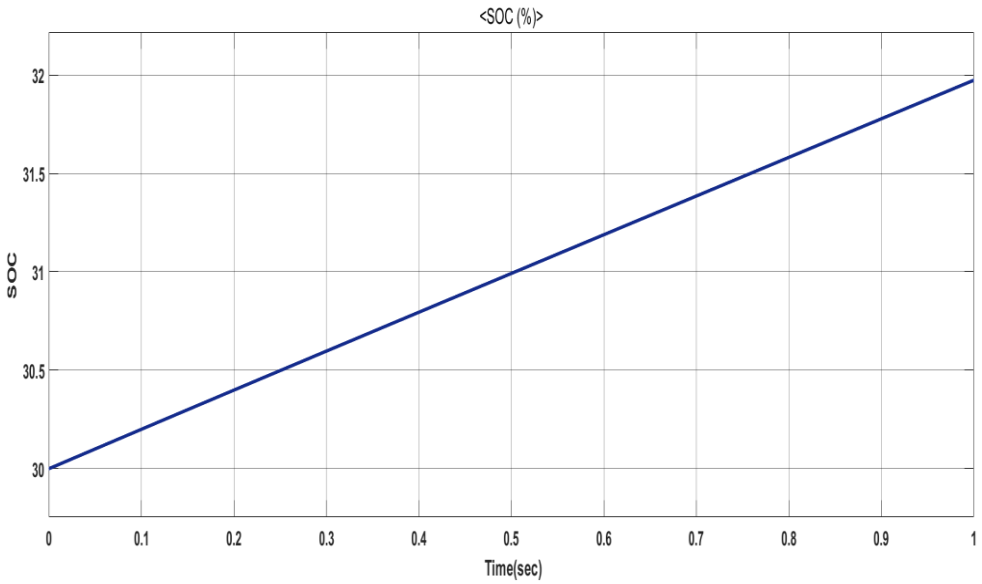

Figure 19: Percentage of SOC

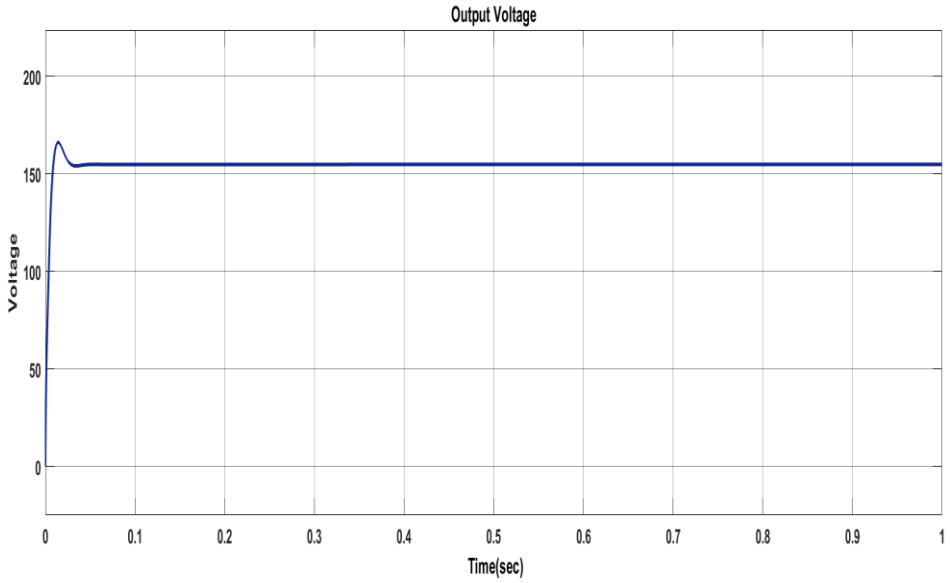

Figure 20: Output Voltage

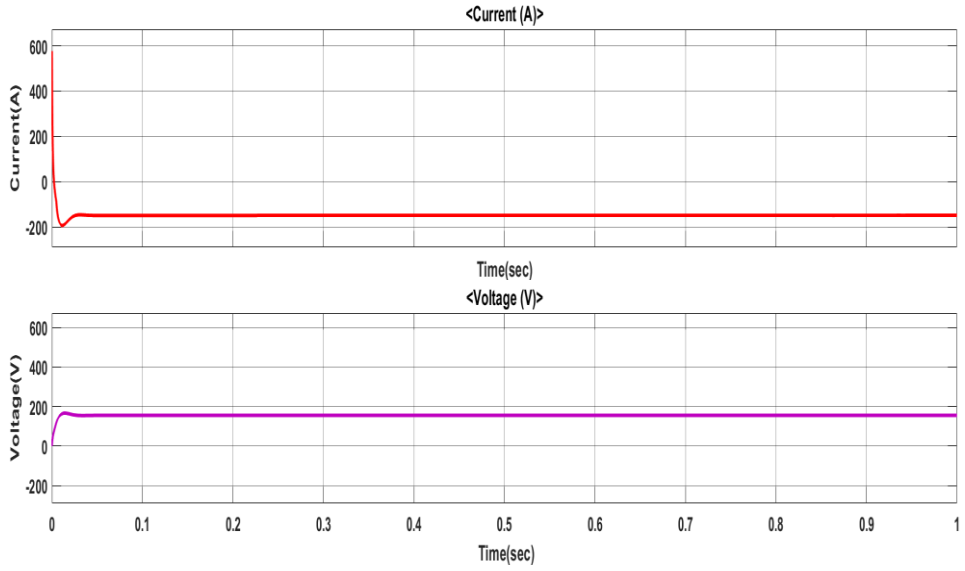

Figure 21: Voltage and Current graphs of lithium ion battery

References

[1] Alber Filba-Martinez, Sergio Busquets-Monge, Joan Nicolas-Apruzzese, and Josep Bordonau. Operating principle and performance optimization of a three-level npc dual-active-bridge dc–dc converter. *IEEE Transactions on Industrial Electronics*, 63(2):678–690, 2016.

[2] Amit Kumar Jain and Rajapandian Ayyanar. Pwm control of dual active bridge: Comprehensive analysis and experimental verification. *IEEE Transactions on Power Electronics*, 26(4):1215–1227, 2011.

[3] Bhimisetty Manoj Kumar, Anupam Kumar, A. H. Bhat, and Pramod Agarwal. Comparative study of dual active bridge isolated dc to dc converter with single phase shift and dual phase shift control techniques. In *2017 Recent Developments in Control, Automation Power Engineering (RDCAPE)*, pages 453–458, 2017.

[4] Alberto Rodríguez Rodríguez Alonso, Javier Sebastian, Diego G. Lamar, Marta M. Hernando, and Aitor Vazquez. An overall study of a dual active bridge for bidirectional dc/dc conversion. In *2010 IEEE Energy Conversion Congress and Exposition*, pages 1129–1135, 2010.

[5] Yanfeng Shen, Huai Wang, Ahmed Al-Durra, Zian Qin, and Frede Blaabjerg. A bidirectional resonant dc–dc converter suitable for wide voltage gain range. *IEEE Transactions on Power Electronics*, 33(4):2957–2975, 2018.